THE ASTROPHYSICAL JOURNAL, 428:483–492, 1994 June 20

FLAT ROTATION CURVES: A RESULT OF THE HELICAL INVERSE CASCADE IN TURBULENT MEDIA?

R. D. PRABHU[1,2] AND V. KRISHAN[1]

Received 1993 February 26; accepted 1993 December 20

ABSTRACT

We have modeled the rotation curves of 21 galaxies observed by Amram et al. (1992), by combining the effects of rigid rotation, gravity, and turbulence. The main motivation behind such modeling is to study the formation of coherent structures in turbulent media and explore its role in the large-scale structures of the universe. The values of the parameters such as mass, turbulent velocity, and angular velocity derived from the rotation curve fits are in good agreement with those derived from the prevalent models.

Subject headings: galaxies: kinematics and dynamics — hydrodynamics — turbulence

1. INTRODUCTION

The rotation curves of galaxies have been the subject of great speculation in the recent past. If galaxies are considered as solid bodies in rotation, then their linear velocity must increase in a linear manner, i.e., $V \propto r$, where r is the radial distance from the center of the galaxy. The trouble arises when the picture of a "falling curve" as predicted by the Newtonian gravity for the outer region of a galaxy does not tally with what is observed. We get a flat rotation curve on the outer scales. This has given birth to many models which try to account for rotation curves. The suggestions include (1) a modification of the Newtonian force (e.g., Milgrom 1983; Milgrom & Bekenstein 1987; Liboff 1992 and references therein), (2) the effect of the magnetic stresses (e.g., Nelson 1988; Battaner et al. 1992 and references therein), and (3) the presence of a large amount of hidden mass that does the trick (e.g., Einasto 1990; Saar 1990 and references therein)!

The issue of dark matter has raised considerable interest in this area, and the gravity of the dark matter appears to be a favorite candidate. This must be tested against its alternatives. Verschuur (1991) has revived the old debate of the missing mass versus the missing physics. The appearance of large-scale structures in turbulent flows (e.g., ter Harr 1989; Moiseev et al. 1983; Frisch, She, & Sulem 1987; Sulem et al. 1989; Moffat 1992; Levich & Tzvetkov 1985; Hasegawa 1985 and references therein) which are stationary, anisotropic, and parity-violating has become an exciting prospect potential enough to play a major role in the astrophysical context. The major weakness of all structure formation models (e.g., CDM; gravitational instability models) up to now is their inability to reproduce the large-scale structures, observed in the universe (of the order of 100 Mpc). Krishan & Sivaram (1991) showed that the clustering and superclustering of galaxies and clusters respectively could be viewed as the outcome of the "inverse cascade" process in a turbulent medium. In this paper we model the flat rotation curves of the galaxies by combining the effects of rigid rotation, gravity, and turbulence.

2. THE INVERSE CASCADE

As reiterated by Scalo, "the properties of the interstellar medium strongly suggest that it is turbulent, in the generalized sense of nonlinear systems which exhibit unpredictable temporal behavior accompanied by self-organizing spatial fluctuations covering a wide range of size scales [Scalo 1987, 349]. ...A particularly interesting type of self-organizing behavior occurs in turbulent fluids in which more than one quantity is conserved, a situation renewed by Hasegawa (1985). In these cases one conserved quantity becomes spatially chaotic by means of a direct cascade from large scales to small scales, while the other self-organizes into large structures by undergoing an inverse cascade from small scales to large scales [Scalo 1987, 371]."

The concept of such an "inverse cascade" is well established for two-dimensional flows in fluids as well as magnetohydrodynamic flows (Kraichnan & Montgomery 1980) The three-dimensional MHD case is also well established. The case for a three-dimensional inverse cascade in fluids is gaining ground with the identification of a new invariant (other than energy) I (defined below), related to the helicity density. Numerous numerical studies are also corroborating the same viewpoint.

The problem of turbulence is addressed in two ways:

1. The Kolmogorov approach, in which we study the statistically stationary states by dimensional arguments. We follow the results of this approach in the present paper (e.g., Levich & Tzvetkov 1985; Krishan & Sivaram 1991).
2. The Navier-Stokes way, in which we look for the solutions of the Navier-Stokes equations hoping that the stationary solutions would comply with the predictions of the former approach (Krishan 1993) (see the Appendix).

2.1. *The Kolmogorov Approach*

Large helicity fluctuations present in a turbulent medium play an essential role in the inverse cascade of energy. The helicity density γ, a measure of the knottedness of the vorticity field $\mathbf{\Omega}$, is defined as

$$\gamma = \mathbf{V} \cdot \mathbf{\Omega} , \quad \mathbf{\Omega} = \nabla \times \mathbf{V} . \tag{1}$$

It is found that the quantity I, defined as

$$I = \int \langle \gamma(x)\gamma(x + r)\rangle d^3x , \tag{2}$$

is also an invariant of an ideal three-dimensional hydrodynamic system in addition to the total energy. On the inclusion of dissipation, these invariants decay differentially. The nature of the nonlinear interaction between the fluid elements is such

[1] Indian Institute of Astrophysics, Bangalore 560034, India.
[2] Also Indian Institute of Science, Bangalore.

that the slow decaying invariant (I, here) cascades toward large spatial scales, and the fast decaying invariant (energy, here) cascades toward smaller spatial scales. By assuming a quasi-normal distribution of helicities, the I-invariant can be expressed as

$$I = \text{const} \int E^2(k) dk \, . \quad (3)$$

Here $E = \int E(k)dk$ is the total energy density.

In the inertial range for the energy invariant we have

$$(kV_k)V_k^2 = \epsilon = V_0^2/\tau \quad (4)$$

where k = wavenumber, V_0 = the initial rms velocity on small scales, τ = the duration for which this energy is available, V_k = velocity in Fourier space, and ϵ = average energy transfer rate per unit mass (ergs g^{-1} s^{-1}). This, combined with $kE(k) = V_k^2$, yields the well-known Kolmogorov spectrum:

$$E(k) = \epsilon^{2/3} k^{-5/3} \, . \quad (5)$$

It would be appropriate to comment on ϵ here. Kolmogorov (1941) conjectured that in a quasi-steady state there should be a stationary flow of energy in the k space from the source to the sink. Thus the energy transfer rate per unit mass should be a constant and be equal to the dissipation rate at the sink. Although numerous experiments have confirmed that ϵ is a strongly fluctuating quantity, surprisingly there is no experimental evidence indicating a deviation from the Kolmogorov spectrum (Levich 1987).

The value of ϵ for the Galaxy has been estimated to be of the order of 8×10^{-3} ergs g^{-1} s^{-1} by considering the various sources (such as supernovae, stellar winds, etc.) which contribute to the turbulence energetics. In the same vein τ is calculated to be 3×10^7 yr (Ruzmaikin, Shukurov, & Sokoloff 1988).

From equation (5), we find total energy $E = \int E(k)dk$

or

$$E(l) = \epsilon^{2/3} l^{2/3} \quad \left(\text{for} \quad k \simeq \frac{1}{l}\right) . \quad (6)$$

The corresponding velocity field may be described as

$$V(l) = (l_z \epsilon)^{1/3} (l/l_z)^{1/3} \quad (7)$$

for some normalizing lenth l_z. Similarly, in the inertial range for the I-invariant, we have

$$(kV_k)[kE^2(k)] = \epsilon' = I_0/\tau \, . \quad (8)$$

where ϵ' = the average mean square helicity density exchange rate between the scales. Combining this with

$$kE(k) = V_k^2 \quad (9)$$

gives

$$E(k) = (I_0/\tau)^{2/5} k^{-1} \, . \quad (10)$$

Or in real space,

$$E(l) = (I_0/\tau)^{2/5} \ln(l/l_z) \quad \text{for} \quad l > l_z \, . \quad (11)$$

Here, the normalizing length l_z can be used to make the transition from one inertial law (eq. [7]) to the other (eq. [11]). The velocity field in this range is described as

$$V(l) = (\epsilon^2 l_z \tau)^{1/5} [\sqrt{\ln(l/l_z)}] \, , \quad (12)$$

where

$$I_0 = V_0^4 l_z \quad (13)$$

which follows from equations (8) and (9).

3. MODELING OF ROTATION CURVES

The complete energy spectrum in a helically turbulent medium derived in Krishan (1991) and Krishan & Sivaram (1991) is reproduced here in Figure 1. In this paper, we model the rotation curves (Figs. 2a–2u) of 21 galaxies observed by Amram et al. (1992), using the Kolmogorov branch $[V(l) \propto l^{1/3}]$ and the flat branch $[V(l) \propto \sqrt{\ln l}]$. We propose a law of velocities which is of the type

$$V(l) = Al + Bl^{1/3} \quad (14)$$

in the inner, i.e., $l \leq l_z$, and

$$V(l) = Cl^{-1/2} + D\sqrt{\ln(l/l_z)} \quad (15)$$

in the outer regions, i.e., $l \geq l_z$ of a galaxy, where A, B, C, and D are the coefficients to be determined from the fits, with the observed velocity fields.

The first terms on the right-hand side of equations (14) and (15) correspond to rigid rotation and gravity, respectively; therefore,

$$A = \omega \, , \quad (16)$$

the angular velocity of a galaxy, and

$$C = \sqrt{GM} \, , \quad (17)$$

(where G is the universal gravitational constant), refers to the mass of a galaxy. The second terms on the right-hand side of equations (14) and (15) are due to the turbulence cascading so that

$$B = \epsilon^{1/3} \quad (18)$$

and

$$D = (\epsilon^2 l_z \tau)^{1/5} \, . \quad (19)$$

By a judicious choice of l_z we can estimate V_0, τ, ϵ, ω, and mass M of a galaxy.

4. RESULTS

The values of V_0, τ, ϵ—the parameters of turbulence—for each of the galaxies are shown in Table 1. The galaxy parameters ω, l_z, and mass M (col. [5]) are shown in Table 2. We have also included the mass (global) M_g (col. [6]) calculated from

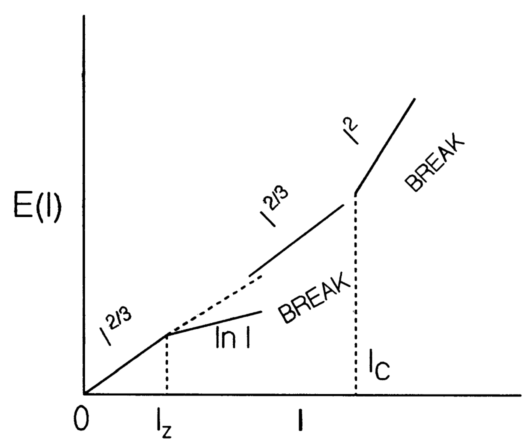

FIG. 1.—Turbulent energy spectrum. l_z, normalizing length; l_c, break due to Coriolis force (Krishan 1991).

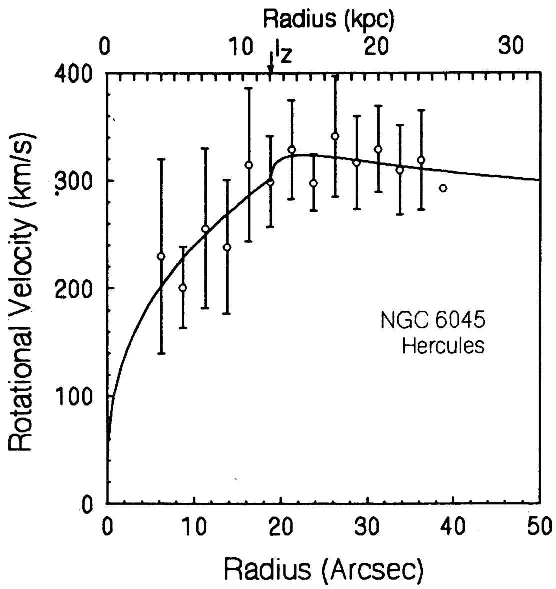

FIG. 2*a*

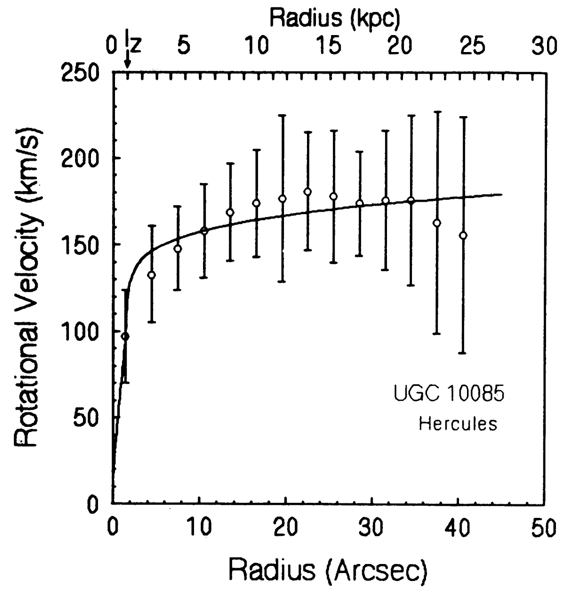

FIG. 2*b*

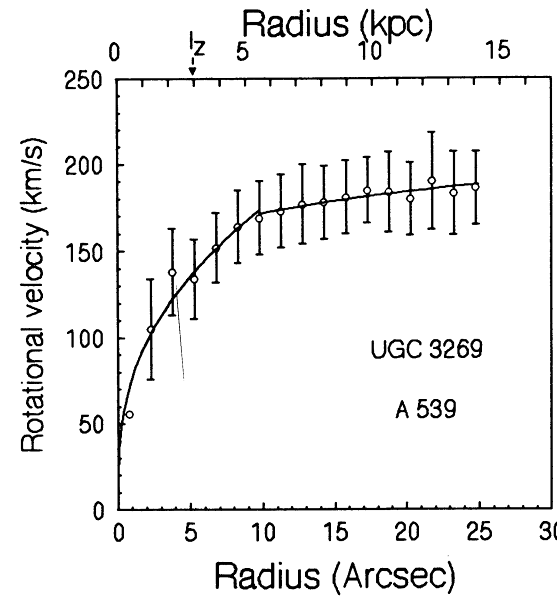

FIG. 2*c*

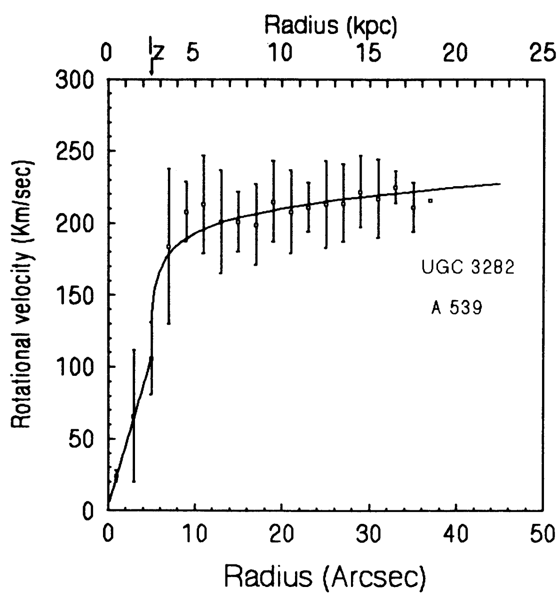

FIG. 2*d*

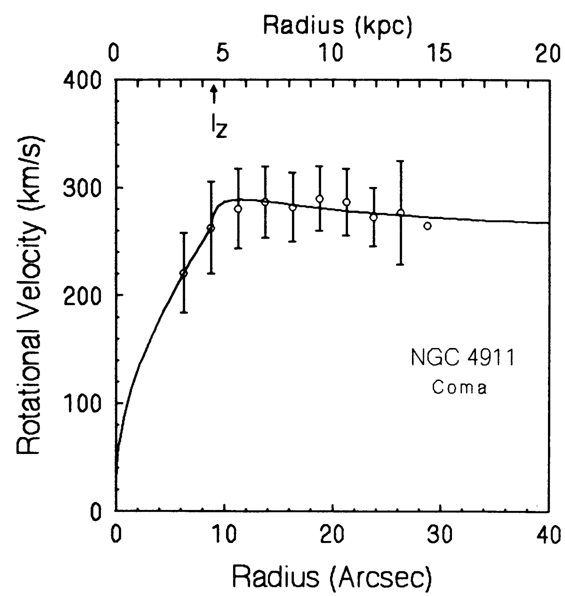

FIG. 2*e*

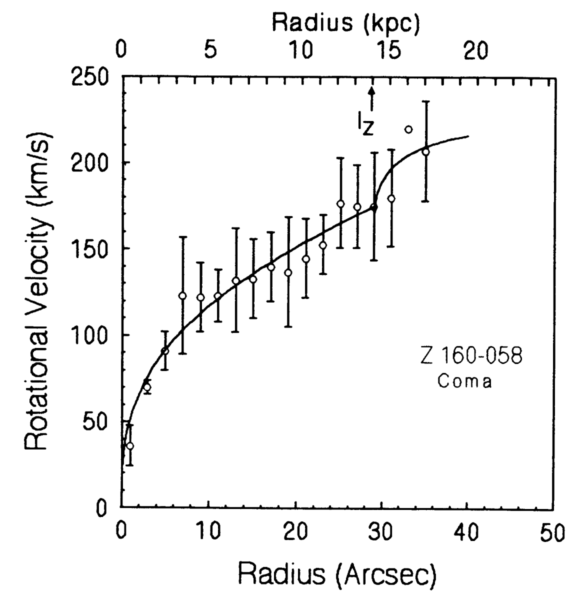

FIG. 2*f*

FIG. 2.—Rotation curves of the galaxies

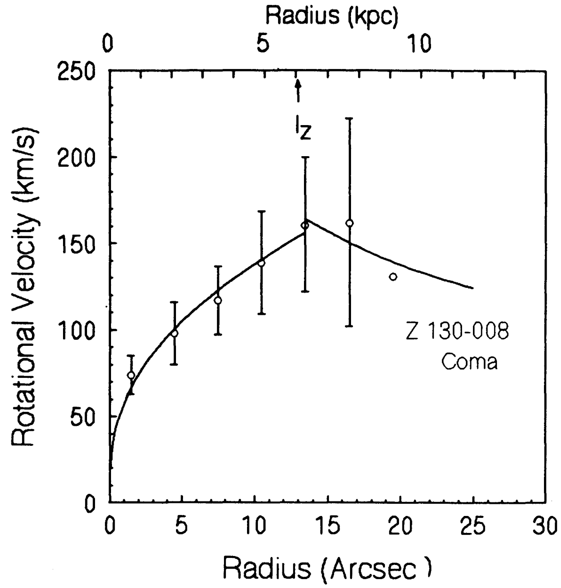

FIG. 2g

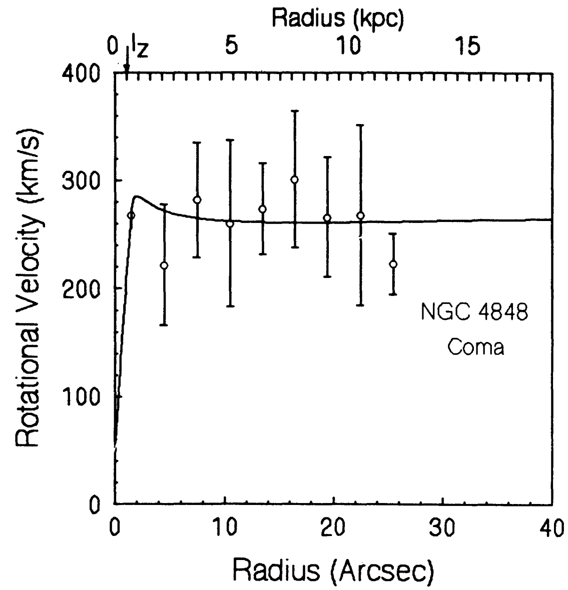

FIG. 2h

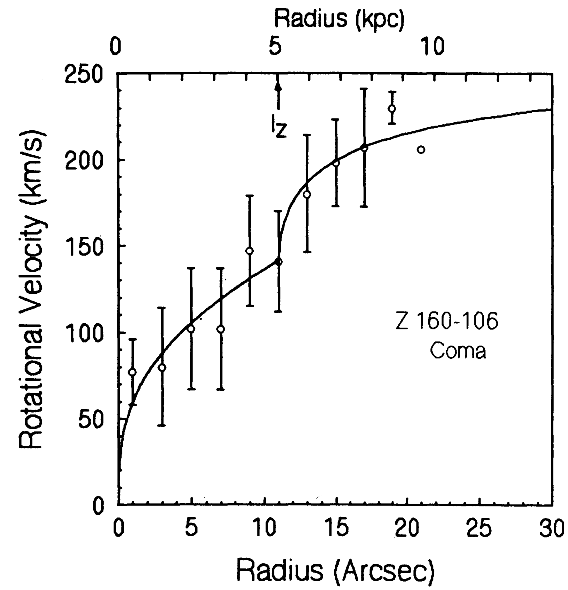

FIG. 2i

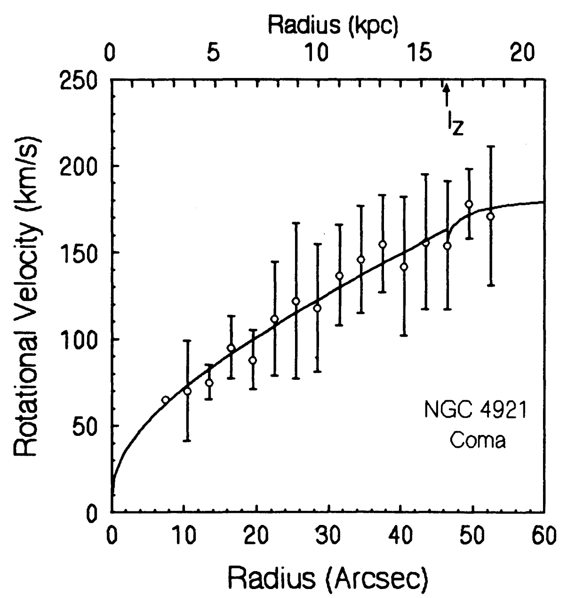

FIG. 2j

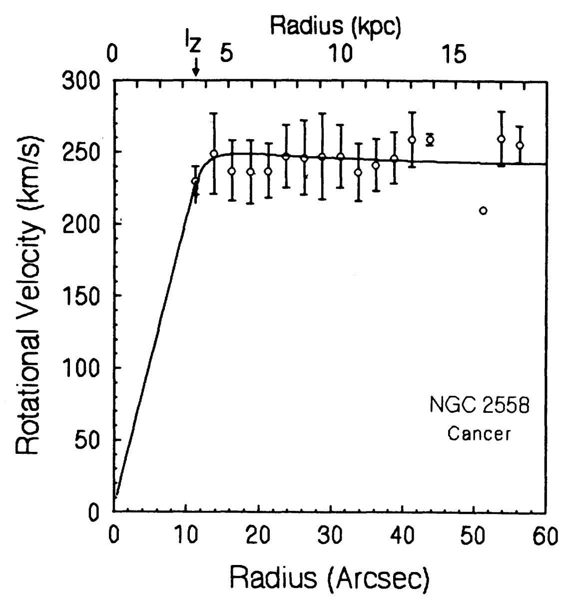

FIG. 2k

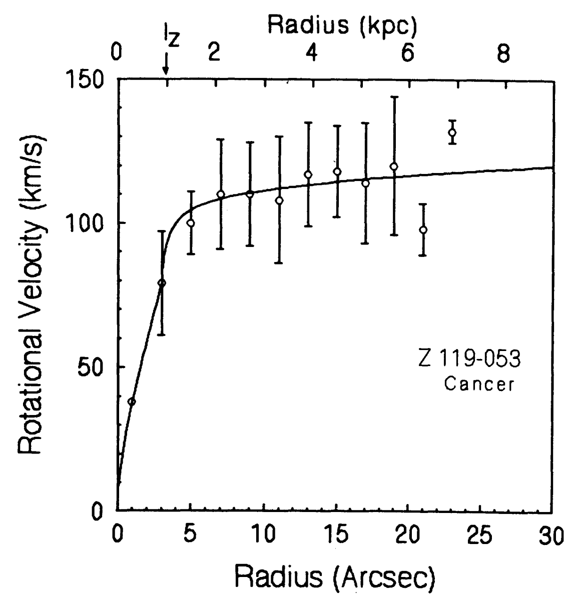

FIG. 2l

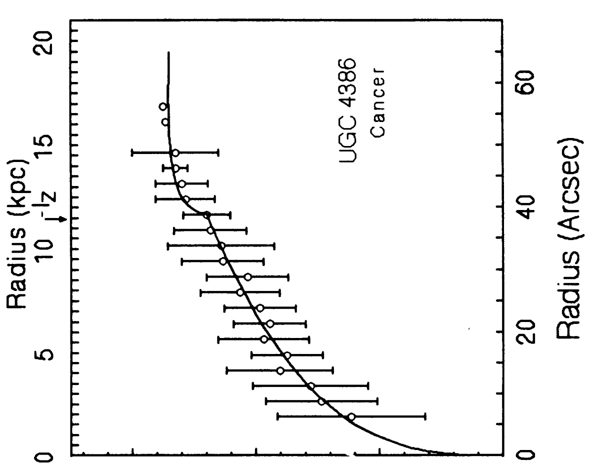

FIG. 2m

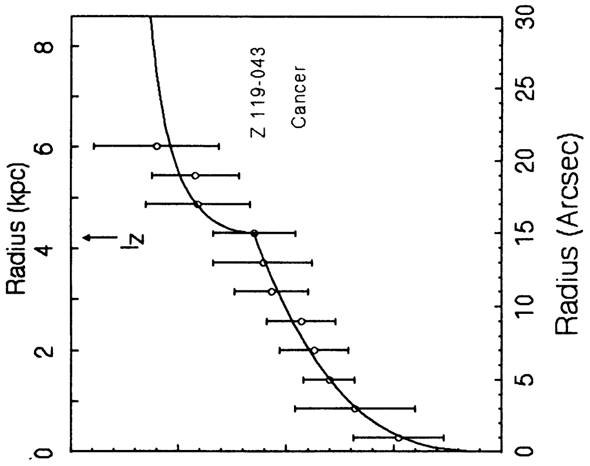

FIG. 2n

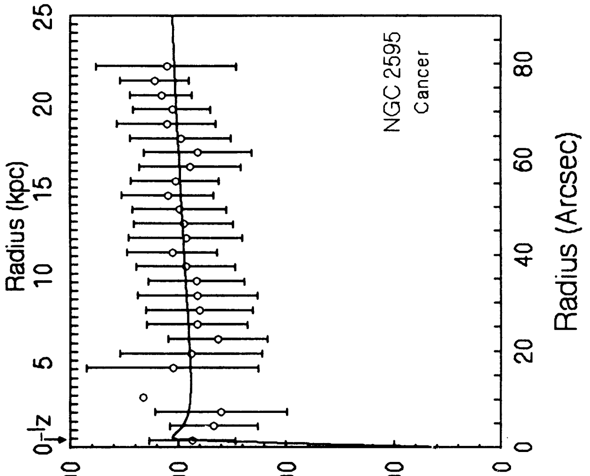

FIG. 2o

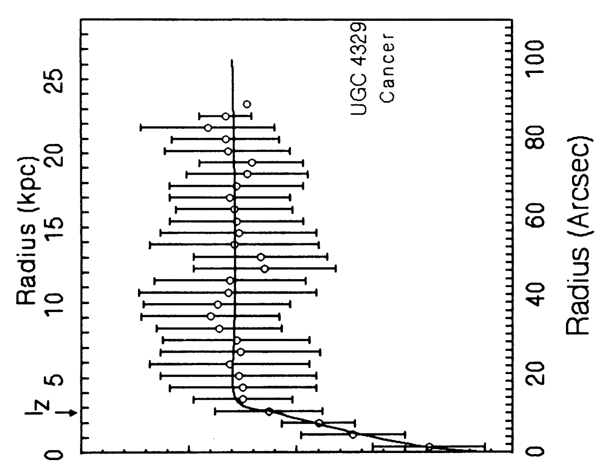

FIG. 2p

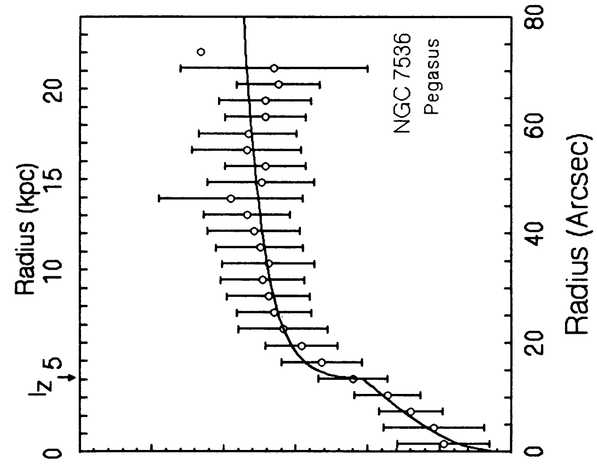

FIG. 2q

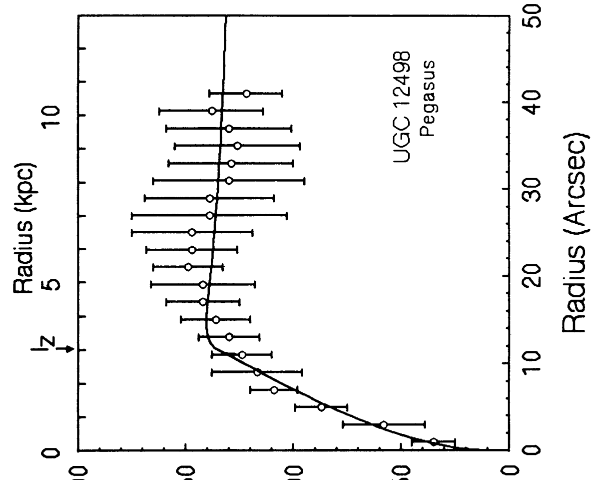

FIG. 2r

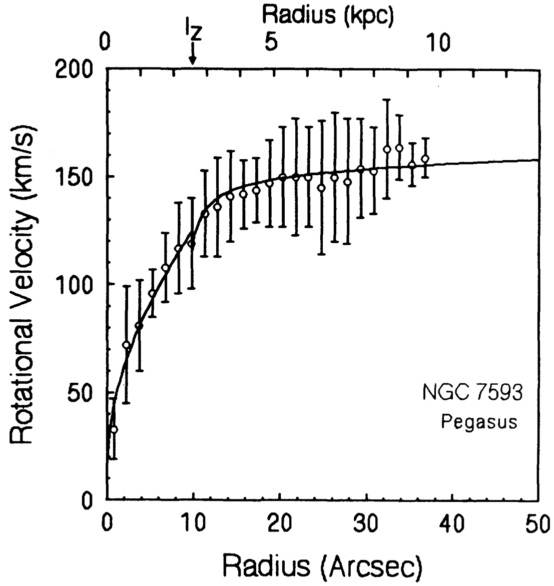

FIG. 2s

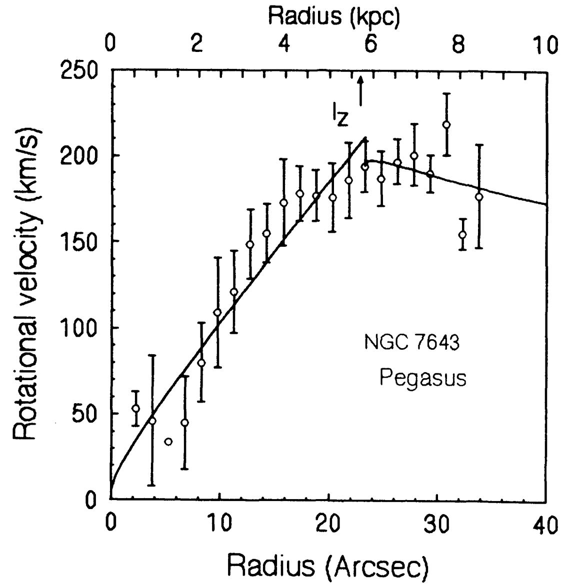

FIG. 2t

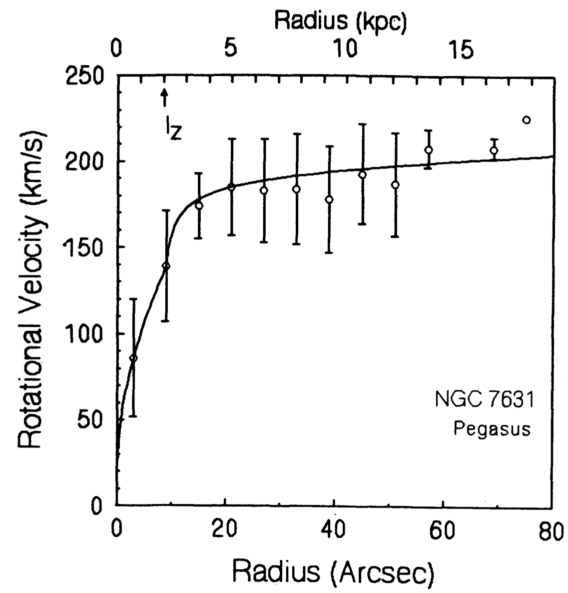

FIG. 2u

TABLE 1

TURBULENCE PARAMETERS

Name (1)	V_0 (km s^{-1}) (2)	τ (10^{13} s) (3)	ϵ (10^{-2} ergs g^{-1} s^{-1}) (4)
Hercules Cluster			
NGC 6045	31.1	1.5	63.4
UGC 10085	338.1	7100	1.6
Abell 539 Cluster			
UGC 3269	85.1	42	17
UGC 3282	8021	3.5×10^8	1.8×10^{-2}
Coma Cluster			
NGC 4911	61.6	8.4	45
Z160−058	86.8	78	9.6
Z130−008	0.026	5.2×10^{-6}	12.9
NGC 4848	156.8	46	53
Z160−106	168.8	180	15.5
NGC 4921	67.8	270	1.7
Cancer Cluster			
NGC 2558	5588	5.1×10^8	6.1×10^{-3}
Z119−053	171.3	2.4×10^3	1.2
UGC 4386	45.9	5.5	38
Z119−043	80.7	59	11
NGC 2595	190.5	37	98
UGC 4329	57.5	94	3.5
Pegasus Cluster			
NGC 7536	210.7	1700	2.5
UGC 12498	41.6	3.6	47
NGC 7593	73.9	47	11.6
NGC 7643	25.5	210	0.3
NGC 7631	106.8	53	21.2

the dark matter model assuming spherical symmetry (Giovanelli & Haynes 1988) and the stellar mass M_S (col. [7]) determined from the stellar models, using M/L ratios (Giovanelli & Haynes 1988; Rubin et al. 1985) and luminosities taken from Amram et al. (1992). The uncertainties in the M/L ratios and in the stellar models have to be taken into account before attempting any comparative study of the various types of masses. We also present the histograms (Figs. 3–9) for each of the quantities mentioned. Our model gives typical values of the various quantities as

$$V_0 \approx 100 \text{ km s}^{-1} ,$$
$$\tau \approx 10^7 \text{ yr} ,$$
$$\epsilon \approx 10^{-2} \text{ ergs g}^{-1} \text{ s}^{-1} ,$$
$$\omega \approx 10^{-16} \text{ s}^{-1} ,$$
$$\text{Mass} \approx 10^{10} M_\odot .$$

One must note that we did not have to choose any abnormal values of l_z for obtaining the best fits and it lies in the range 2–10 kpc. This tells us that on scales smaller than l_z, the turbu-

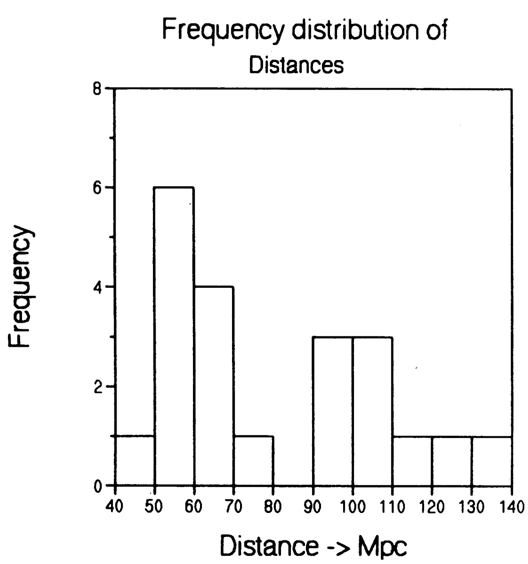

FIG. 3.—Histogram for distance

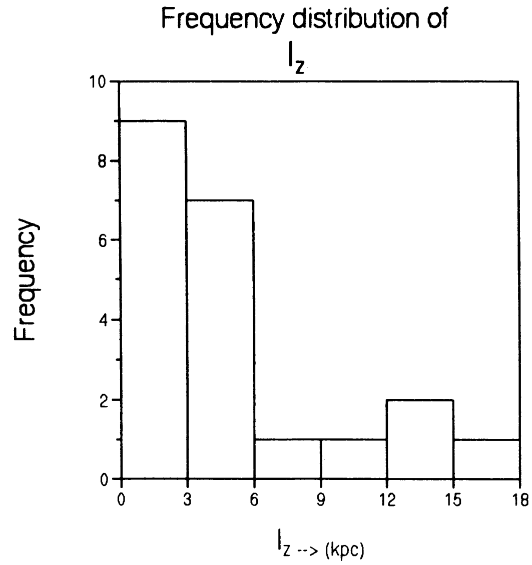

FIG. 4.—Histogram for l_z

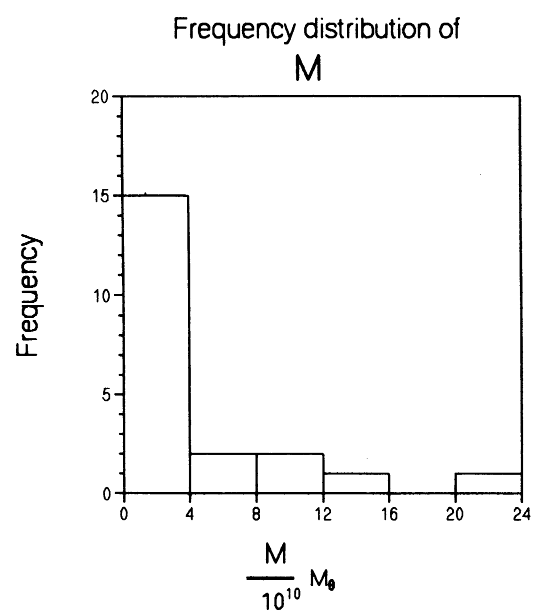

FIG. 5.—Histogram for M

TABLE 2

VALUES OF ω, l_z, AND MASS

Name (1)	Distance (Mpc) (2)	l_z (Kpc) (3)	ω ($10^{-16}\,s^{-1}$) (4)	M ($10^{10}\,M_\odot$) (5)	M_g[a] ($10^{10}\,M_\odot$) (6)	M_s[b] ($10^{10}\,M_\odot$) (7)
			Hercules Cluster			
NGC 6045	133.1	12.0	0.4	23.7	4.5	1.7
UGC 10085	129.6	0.9	21.9	0.2	5.8	2.3
			Abell 539 Cluster			
UGC 3269	118.7	3.0	3.0	1.0	12.3	5.5
UGC 3282	109.6	2.6	12.4	0.9	6.0	2.3
			Coma Cluster			
NGC 4911	105.5	4.4	5.9	6.6	16.9	7.5
Z160−058	100.8	14.0	0.3	8.9	2.9	1.1
Z130−008	96.6	6.2	1.2	3.6	1.4	0.5
NGC 4848	95.5	0.6	94.0	0.8	15.8	7.9
Z160−106	94.6	4.9	0.6	2.0	5.1	2.6
NGC 4921	72.6	16.2	1.4	8.6	17.5	8.7
			Cancer Cluster			
NGC 2558	66.6	3.6	20.4	3.6	8.5	4.2
Z119−053	64.6	0.9	16.6	0.1		
UGC 4386	61.7	11.4	0.1	14.6	6.3	2.8
Z119−043	59.3	4.2	0.07	1.2		
NGC 2595	57.6	0.4	151.1	0.6	6.0	2.3
UGC 4329	54.4	2.7	5.6	0.7	1.8	0.7
			Pegasus Cluster			
NGC 7536	62.5	4.0	2.8	0.9	5.9	2.6
UGC 12498	55.6	2.9	6.4	1.0	2.9	1.3
NGC 7593	54.7	2.5	3.9	0.6	1.6	0.6
NGC 7643	51.1	5.7	10.0	4.7	1.7	0.6
NGC 7631	49.9	2.1	4.5	0.7	4.9	2.2

[a] Global mass from dark matter model.

[b] Mass in the stars (derived from assuming the global M/L ratios of each of the morphological types; Giovanelli & Haynes 1988).

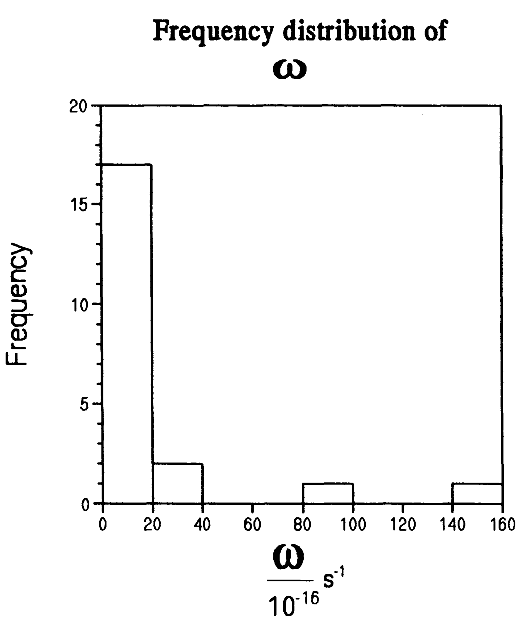

FIG. 6.—Histogram for ω

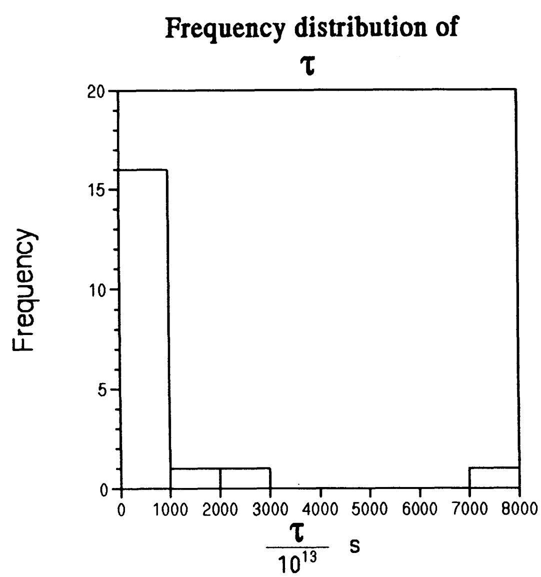

FIG. 7.—Histogram for τ. Note that the values for UGC 3282 and NGC 2558 have been rejected.

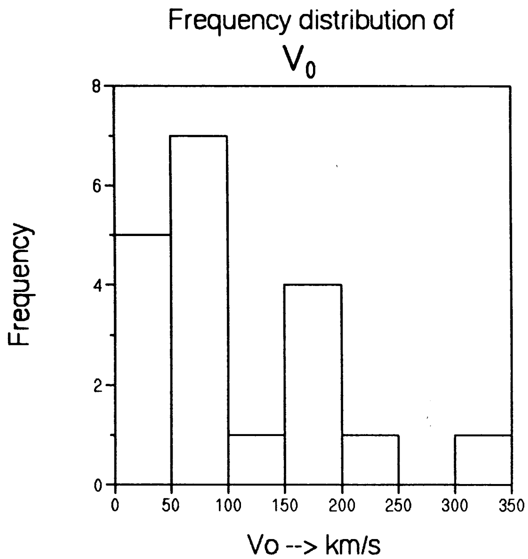

FIG. 8.—Histogram for V_0. The V_0 for UGC 3282 and NGC 2558 have been rejected.

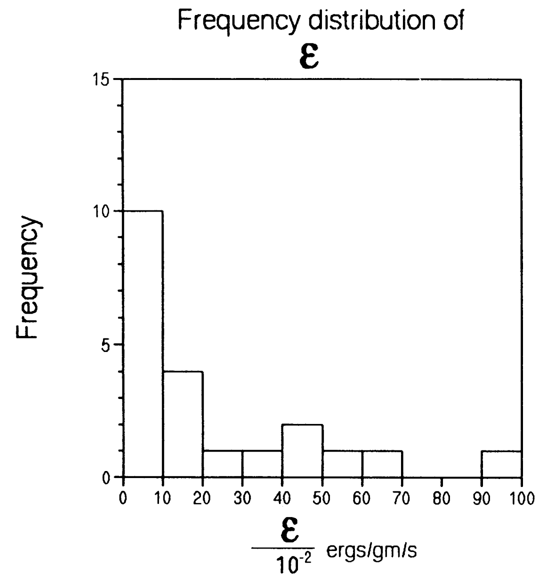

FIG. 9.—Histogram for ϵ

lence is isotropic and on the scales equal to and larger than l_z the turbulence becomes more and more anisotropic facilitating the inverse cascade of energy. We find two odd ones out in our sample of 21 galaxies, viz., UGC 3282 and NGC 2558. They have exceptionally large values of the turbulent velocity V_0 and exceptionally small values of the energy injection rate parameter ϵ. We shall look out for more such cases in other data sets and examine if the peculiarities earn these galaxies a separate class.

5. CONCLUSIONS

The velocity-radius relation has been derived using Kolmogorov arguments. We find that the matter at a large radius exhibits a balance of hydrodynamic forces, i.e., dynamical pressure, and Reynolds stress—produced by the forced small-scale flow—without the necessity of invoking a gravitational force, generated out of a mass distribution of the type $M \propto r$. In other words, our system is hydrodynamically bound.

We also find that ϵ and τ values for each of the galaxies obtained by us are almost of the same order as that quoted for our Galaxy (Ruzmaikin et al. 1988). Therefore it appears possible to model the observed rotation curves of the galaxies by suitably combining the effects of rigid rotation, gravity, and turbulence. The validity of the "turbulence model" can be further substantiated by confronting it with the observations of the velocity fields on the larger scales like clusters and superclusters.

APPENDIX

We have given Kolmogorov arguments to explain the "inverse cascade" concept. Alternately the theory of generation of large-scale structures in three-dimensional flows lacking parity invariance has its analog in the α effect which explains the generation of large-scale magnetic fields. The formation of large-scale structures can be viewed as the manifestation of long-wavelength instability of the corresponding small-scale flow. To get a flavor of the physical processes involved, we study the Navier-Stokes equation for the small- and large-scale motion to understand their interplay. Given below is the analysis due to Frisch et al. (1987) which has been generalized to include the expansion of the fluid by Krishan (1993).

The initial small-scale flow $\boldsymbol{u}^{(0)}(\boldsymbol{r}, t)$ with an anisotropic forcing $\boldsymbol{f}$ satisfies the Navier-Stokes equation, as well as the incompressibility condition:

$$\partial_t u_i^{(0)} + \partial_j(u_i^{(0)} u_j^{(0)}) = -\partial_i p^{(0)} + \nu \nabla^2 u_i^{(0)} + f_i \,. \tag{A1}$$

We then perturb the basic flow $\boldsymbol{u}^{(0)} \to \boldsymbol{u}$, where $\boldsymbol{u}$ has nontrivial large-scale component $\boldsymbol{w} = \langle \boldsymbol{u} \rangle$. The small-scale flow $\tilde{\boldsymbol{u}} = \boldsymbol{u} - \boldsymbol{w}$ is advected by the mean flow and therefore satisfies

$$\partial_t \tilde{u}_i + w_j \partial_j \tilde{u}_i + \partial_j(\tilde{u}_i \tilde{u}_j) = -\partial_i \tilde{p} + \nu \nabla^2 \tilde{u}_i + f_i \tag{A2}$$

while finding the solution of equation, (A2) $\boldsymbol{w}$ is considered to be uniform and constant. The large-scale flow satisfies

$$\partial_i w_i + \partial_j(w_i w_j + R_{ij}) = -\partial_i p + \nu \nabla^2 w_i \,, \tag{A3}$$

where $R_{ij} = \langle u_i u_j \rangle$ are the average small-scale Reynolds stresses. Notice that R_{ij} becomes w-dependent and, thereby, contributes to the dynamics of the large-scale flow. To solve for the large-scale flow we (1) solve for the small-scale flow, (2) calculate the mean small-scale Reynolds stresses; and (3) substitute R_{ij} in equation (A3).

Frisch et al. (1987) considered a flow $\tilde{\boldsymbol{u}}_i$ obtained with the force $\boldsymbol{f}$, of the form

$$f_1 = \frac{\nu V_0 \sqrt{2}}{l_0^2} \cos\left(\frac{y}{l_0} + \frac{\nu t}{l_0^2}\right),$$
$$f_2 = \frac{\nu V_0 \sqrt{2}}{l_0^2} \cos\left(\frac{y}{l_0} - \frac{\nu t}{l_0^2}\right), \quad \text{(A4)}$$
$$f_3 = f_1 + f_2,$$

where l_0 is the characteristic spatial scale of the basic flow. It is found that equation (A3) admits solutions of the form

$$\psi = w_1 + i w_2 = e^{ikz} e^{(\alpha k - \nu k^2)t}$$

where

$$\alpha = \frac{V_0^2 l_0}{2\nu} = \left(\frac{1}{2}\right) R V_0$$

(R being the Reynolds number for the flow; $R = V_0 l_0/\nu$). For wavenumbers k such that $\alpha k > \nu k^2$, the modes grow and a large-scale flow results. This is refered to as the AKA instability (anisotropic kinetic alpha effect). Recently Krishan has generalized the above treatment by including expansion of the fluid and suggested this as a possible way of explaining the large-scale structures observed in the universe (Krishan 1993). The rotating galaxy, with its supernova explosions, stellar winds, etc.—providing the necessary forcing at "small scales"—may provide the appropriate setting for such large-scale flows to develop. Thus, the role played by the small-scale Reynolds stresses is no mean one. They effectively provide the support for motion on large scales. Turbulence, being no longer isotropic on these scales, is tamed by this phenomena of "self-organization."

Further investigations of the above phenomena including compressibility effects, etc. are underway.

REFERENCES

Amram, P., et al. 1992, A&AS, 94, 175
Battaner, E., et al. 1992, Nature, 360, 652
Einasto, J. 1990, Australian J. Phys., 43, 123
Frisch, U., She, Z. S., & Sulem, P. L. 1987, Physica, 28D, 382
Giovanelli, R., & Haynes, M. P. 1988, in Galactic and Extragalactic Radio Astronomy, ed. G. L. Verschuur & K. I. Kellermann (Berlin: Springer-Verlag), 537
Hasegawa, A. 1985, Adv. Phys., 34, 1
Kolmogorov, A. N. 1941, Dokl. Akad. Nauk SSSR, 30, 299
Kraichnan, R. H., & Montgomery, D. 1980, Rep. Prog. Phys., 43, 5
Krishan, V. 1991, MNRAS, 250, 50
———. 1993, MNRAS, 264, 257
Krishan, V., & Sivaram, C. 1991, MNRAS, 250, 157
Levich, E. 1987, Phys. Rep., 151 (3–4), 129
Levich, E., & Tzvetkov, E. 1985, Phys. Rep., 128, 1
Liboff, R. 1992, ApJ, 397, L71
Milgrom, M. 1983, ApJ, 270, 365
Milgrom, M., & Bekenstein, J. 1987, in IAU Symp. 117, Dark Matter in the Universe, ed. J. Kormendy & G. R. Knapp (Dordrecht: Reidel), 319
Moffat, H. K. 1992, Ann. Rev. Fluid Mech., 24, 281
Moiseev, S. S., et al. 1983, Sov. Phys. JETP, 58 (6), 1149
Nelson, A. H. 1988, MNRAS, 233, 115
Rubin, V. C., Burstein, D., Ford, W. K., Jr., & Thonnard, N. 1985, ApJ, 289, 81
Ruzmaikin, A. A., Shukurov, A. M., & Sokoloff, D. D. 1988, Magnetic Fields of Galaxies (Dordrecht: Kluwer), 150
Saar, E. 1990, Australian J. Phys., 43, 159
Scalo, J. M. 1987, in Interstellar Processes, ed. D. J. Hollenbach & H. A. Thronson, Jr. (Dordrecht: Reidel), 349
Sulem, P. L., She, Z. S., Scholl, H., & Frisch, U. 1989, J. Fluid Mech., 205, 341
ter Harr, D. 1989, Phys. Scripta, 39, 731
Verschuur, G. L. 1991, Comment Ap., 15 (4), 189